

AD-A069 618

NAVAL RESEARCH LAB WASHINGTON DC

F/G 9/1

ANALYTIC SCALING OF EFFICIENCY FOR THE GYROTRON TRAVELLING WAVE--ETC(U)

MAY 79 K R CHU, A T DROBOT, H H SZU

MIPR-FY61970026

NRL-MR-3892

NL

UNCLASSIFIED

| OF |

AD
40896/B

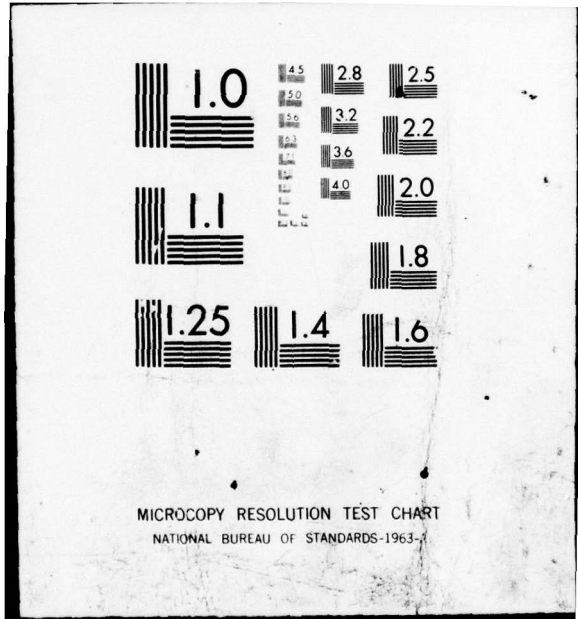


END
DATE
FILMED

7-79

DDC





MICROCOPY RESOLUTION TEST CHART
NATIONAL BUREAU OF STANDARDS-1963-A

12⁵¹

NRL Memorandum Report 3892

LEVEL II

ADA 069618

Analytic Scaling of Efficiency for the Gyrotron Travelling Wave Amplifier Operating at Cyclotron Harmonics

K. R. CHU

Plasma Physics Division

A. T. DROBOT

*Science Applications, Inc.
McLean, Virginia 22101*

H. H. SZU

Plasma Physics Division

AND

P. SPRANGLE

Plasma Physics Division

DDC
RECEIVED
JUN 11 1979

[Handwritten initials]

May 15, 1979



NAVAL RESEARCH LABORATORY
Washington, D.C.

Approved for public release; distribution unlimited.

70 06 08 013

REPORT DOCUMENTATION PAGE		READ INSTRUCTIONS BEFORE COMPLETING FORM
1. REPORT NUMBER NRL Memorandum Report 3892	2. GOVT ACCESSION NO.	3. RECIPIENT'S CATALOG NUMBER
4. TITLE (and Subtitle) ANALYTIC SCALING OF EFFICIENCY FOR THE GYROTRON TRAVELLING WAVE AMPLIFIER OPERATING AT CYCLOTRON HARMONICS,	5. TYPE OF REPORT & PERIOD COVERED Interim report on a continuing NRL problem	
7. AUTHOR(s) K. R. Chu, A. T. Drobot*, H. H. Szu and P. Sprangle	8. CONTRACT OR GRANT NUMBER(s) 62762N	
9. PERFORMING ORGANIZATION NAME AND ADDRESS Naval Research Laboratory Washington, DC 20375	10. PROGRAM ELEMENT, PROJECT, TASK AREA & WORK UNIT NUMBERS NRL Problem R18-10 & R08-92 MIPR No. FY61970026 Subtask XF54-581-007	
11. CONTROLLING OFFICE NAME AND ADDRESS Rome Air Development Center/OCTP, Griffiss AFB, NY 13441 and Naval Electronic Systems Command/304, Washington, DC 20360	12. REPORT DATE May 15, 1979	
14. MONITORING AGENCY NAME & ADDRESS (if different from Controlling Office) 15 May 79	13. NUMBER OF PAGES 12	
16. DISTRIBUTION STATEMENT (of this Report) Approved for public release; distribution unlimited. 12 13 p. 16 F54581		15. SECURITY CLASS. (of this report) UNCLASSIFIED
17. DISTRIBUTION STATEMENT (of the abstract entered in Block 20, if different from Report) 14 NRL-MR-3892 17 XF54581007		15a. DECLASSIFICATION/DOWNGRADING SCHEDULE
18. SUPPLEMENTARY NOTES This work was supported by Rome Air Development Center, MIPR No. FY761970026. *Science Applications, Inc., McLean, VA 22101 Ballistic Missile Defense Advanced Technology Center, Huntsville, Ala. 35807, NRL Problem R08-95 (Continues)		
19. KEY WORDS (Continue on reverse side if necessary and identify by block number) Analytic scaling Gyrotron travelling wave amplifier Cyclotron harmonics 15 MIPR-FY61970026		
20. ABSTRACT (Continue on reverse side if necessary and identify by block number) An analytical expression for the efficiency of the gyrotron travelling wave amplifier is derived for the case of nonfundamental cyclotron harmonic operation. It scales the efficiency with respect to the modes and parameters of operation and gives the conditions for optimum performance. 2.52 950		

18. Supplementary Notes (Continued)

MIPR No. W31RPD-93-Z082 and Naval Electronic Systems Command, XF54-581.

Accession For	
NTIS GINA&I	<input checked="" type="checkbox"/>
DDC TAB	<input type="checkbox"/>
Unannounced	<input type="checkbox"/>
Justification	
By _____	
Distribution/	
Availability Codes	
Dist	Avail and/or special
A	

An interesting electromagnetic radiation mechanism¹⁻³ known as the electron cyclotron maser has been the subject of intense research activities in recent years. This mechanism has been the basis for a new class of microwave devices called gyrotrons capable of generating microwaves at unprecedented power levels at millimeter and submillimeter wavelengths. A detailed description of the cyclotron maser mechanism is given in Reference 4, and brief summaries of gyrotron theories and experiments together with lists of references can be found in recent review papers.^{5,6}

In the present study, we will concentrate on a particular type of gyrotrons--the gyrotron travelling wave amplifier (gyro-TWA). The basic physical processes taking place in a gyro-TWA have been analyzed in recent linear and nonlinear theories.^{4,7-12} In the actual operation of a gyro-TWA, the beam-to-wave energy conversion efficiency is perhaps the most important consideration. References 10-13 contain detailed studies of the saturation mechanisms and calculations of efficiency for the operation at the fundamental cyclotron harmonic. However, the scaling of the efficiency with respect to the various modes and parameters of operation has not been considered in any detail, nor has the operation at the nonfundamental cyclotron harmonics. The nonfundamental harmonic operation is of great importance for the amplification of submillimeter waves if unrealistically high magnetic fields (> 100 kG) are to be avoided. In anticipation of the growing experimental effort aimed at the generation of submillimeter waves, our main purpose in the present study is to derive a general analytical expression for the operating efficiency.

Derivation of a general dispersion relation. The typical configuration of a gyro-TWA consists of an annular electron beam propagating inside a waveguide of circular cross-section (of radius r_w). The electrons, guided

Note: Manuscript submitted March 22, 1979.

by a uniform magnetic field ($B_0 \hat{e}_z$), move along helical trajectories. In our model, all the beam electrons have the same perpendicular velocity (v_{10}), and also the same parallel velocity (v_{z0}), with their guiding centers uniformly distributed on a surface of constant radius r_0 (see Figure 1). We assume that the beam is sufficiently tenuous that its space charge electric field can be neglected, and the spatial structure of the vacuum waveguide mode is unaffected by the presence of the beam. The beam interacts with a single TE_{mn} waveguide mode, where m and n are, respectively, the azimuthal and radial eigenmode numbers. The dynamics of the electron beam is described by the linearized relativistic Vlasov equation which couples with the Maxwell equations to form a complete set. Methods for obtaining the dispersion relation from this set of coupled equations are standard.⁷ Here we present the result directly.

$$\frac{\omega^2}{c^2} - k_z^2 - x_{mn}^2/r_w^2 = \frac{-4\nu}{\gamma_0^2 r_w^2 K_{mn}} \left\{ \frac{\left(\omega^2 - k_z^2 c^2 \right) \beta_{10}^2 H_{sm} \left(x_{mn} r_0/r_w, x_{mn} r_L/r_w \right)}{\left[\omega - k_z v_{z0} - s\Omega_c \right]^2} - \frac{\left(\omega - k_z v_{z0} \right) Q_{sm} \left(x_{mn} r_0/r_w, x_{mn} r_L/r_w \right)}{\left[\omega - k_z v_{z0} - s\Omega_c \right]} \right\}, \quad (1)$$

where $\beta_{10} = v_{10}/c$, $\Omega_c = eB_0/\gamma_0 mc$, $r_L = v_{10}/\Omega_c$, x_{mn} is the n -th root of $J'_m(x) = 0$, $J_m(x)$ is the Bessel function of order m , $J'_m(x) = dJ_m(x)/dx$, $\nu \equiv Ne^2/mc^2$ is a dimensionless beam density parameter, N is the number of electrons per unit axial length, and the functions K_{mn} , H_{sm} , Q_{sm} are defined as follows: $K_{mn} = J_m^2(x_{mn}) - J_{m-1}(x_{mn})J_{m+1}(x_{mn})$, $H_{sm}(x,y) =$

$$\left[J_{s-m}(x) J'_s(y) \right]^2, \text{ and } Q_{sm}(x,y) = 2H_{sm}(x,y) + y \left[J_{s-m}^2(x) J'_s(y) J''_s(y) + \frac{1}{2} J_{s-m-1}^2(x) J'_s(y) J'_{s-1}(y) - \frac{1}{2} J_{s-m+1}^2(x) J'_s(y) J'_{s+1}(y) \right]. \quad \text{The dispersion relation}$$

in Equation (1) is more general than those found in literature in that the waveguide mode numbers m , n , and the cyclotron harmonic number s are all treated as free parameters. This will provide the option to analyze all possible interactions as one searches for the optimum efficiency. On the right-hand side of Equation (1), the first term is the source of the instability, while the second term imposes a threshold beam energy for the instability. For the nonfundamental harmonics ($s > 1$), it can be shown that the threshold energy (typically below 1 keV) is much lower than the typical beam energy (tens of keV); hence the second term can be neglected.

Substituting $\omega = \omega_0 + \Delta\omega$, $k_z = k_{z0}$ into Equation (1), where (ω_0, k_{z0}) is the point at which the waveguide characteristic curve

$$\omega^2 - k_z^2 c^2 - \frac{x^2}{mn} c^2 / r_w^2 = 0 \quad (2)$$

intersects with the beam characteristic curve

$$\omega - k_z v_{z0} - s\Omega_c = 0 \quad (3)$$

we can easily evaluate $\Delta\omega (= \Delta\omega_r + i\Delta\omega_i)$, with the result

$$\Delta\omega_r = \left[\frac{v_x^2 \frac{H_{sm}^2 \omega_0^2 c^4}{mn s m^2 \omega_0^2}}{4\gamma_0^2 K_{mn}^2 \omega_0^4 r_w^4} \right]^{1/3} \quad \text{and} \quad \Delta\omega_i = \sqrt{3} \Delta\omega_r \quad (4)$$

In Equation (4), $\Delta\omega_r$ gives the frequency width for resonant beam-wave interaction, and $\Delta\omega_i$ gives the growth rate.

Numerical simulations. The preceding linear analysis has been complemented by a single-wave numerical simulation code¹³ developed to simulate the amplification of azimuthally symmetric modes at the nonfundamental harmonic frequency. The simulation shows two different but simultaneously present saturation mechanisms--depletion of free electron energy and loss

of phase synchronism. The first mechanism dominates when the beam energy is slightly above threshold. Saturation occurs as soon as the beam loses a small amount of energy and the system becomes linearly stable. The second mechanism dominates when the beam energy is well above the threshold. Saturation occurs because an average electron loses so much energy that its relativistic cyclotron frequency no longer matches the wave frequency to favor unstable interactions. Figure 2 shows a typical efficiency curve as a function of time. It increases at the linear growth rate, then exhibits an oscillatory behavior after saturation. As found in Reference 11, both mechanisms are important for the fundamental cyclotron harmonic interaction. However, there is a basic difference between the fundamental and nonfundamental harmonic interactions; namely, for the latter interaction, we find that the threshold beam energy is typically so low that the energy depletion saturation mechanism can be disregarded. This has allowed us to derive an analytical scaling relation for the efficiency.

Efficiency scaling relation. For the purpose of efficiency optimization in the multiple parameter space typical of a gyro-TWA system an analytical scaling relation is essential. Without loss of generality, we shall derive the efficiency scaling relation in the beam reference frame (i.e., the frame in which $v_{z0} = 0$), and denote the beam frame quantities with a prime. A simple Lorentz transformation^{11,12} can be used to convert the beam frame efficiency into lab frame efficiency. In order to minimize the possibility of spurious oscillations, it is advantageous to choose a magnetic field such that Eqs. (2) and (3) intersect at only one point (i.e. at a grazing angle). In the beam frame, this implies

$$\omega'_0 = s \Omega'_c = \frac{x_{\text{min}} c}{r_w} \quad (5)$$

Henceforth, our analysis will be restricted to this particular case.

In the linear analysis, we have shown that the following condition holds at the onset of the instability,

$$\omega_r' - s \Omega_e' / \gamma_0' = \Delta\omega_r' \quad (6)$$

where $\Omega_e' = eB_0/mc$ and $\Delta\omega_r'$ is a positive quantity given by Equation (4). As the instability evolves, the average energy of the electrons decreases, hence the left-hand side of Equation (6) also decreases. Knowing this tendency and the width for resonant interaction, we expect the following condition to hold at the saturation state,

$$\omega_r' - s \Omega_e' / \langle \gamma_s' \rangle \approx -\Delta\omega_r' \quad (7)$$

where $\langle \gamma_s' \rangle$ is the average γ' of all the electrons at saturation. This is the physically expected saturation condition because any further decrease in electron energy would shift the electron cyclotron frequency out of the range for resonant beam-wave interaction. Equation (7) was found to be in good agreement with our extensive simulation data.

From Equations (4) - (7) and assuming $\Delta\omega_r' \ll \omega_0'$, we obtain an approximate estimate for the efficiency η' ,

$$\eta' \equiv \frac{\gamma_0' - \langle \gamma_s' \rangle}{\gamma_0' - 1} \approx \frac{1}{\gamma_0' - 1} \left[\frac{2v' \gamma_0'^2 H_{sm} (x_{mn} r_0 / r_w, x_{mn} r_L / r_w) \beta_{10}'^2}{K_{mn} x_{mn}^2} \right]^{1/3} \quad (8)$$

where H_{sm} , K_{mn} , and x_{mn} are all frame independent quantities.

Equation (8) shows how η' scales with the mode numbers m , n , s , and the operating parameters, v' , γ_0' , and r_0 . Note that η' is independent of the waveguide radius r_w . The scaling of η' with respect to v' is especially simple; namely, $\eta' \propto v'^{1/3}$. For a given mode of operation, the choice of r_0 should be such that H_{sm} falls on or near its peak value. Scaling of η' with respect to m , n , s , and γ_0' is more complicated and can best be seen through numerical plots of Equation (8). Some examples are shown in Figure 3, in which η' is

is plotted (in continuous curves) against the beam energy (γ_0') for $m=0$, $s=n=2, 3$, and 4 . In each case the beam position (r_0) has been chosen to maximize H_{sm} . It is seen that higher cyclotron harmonics generally give lower efficiency, as expected, and the behavior of η' as a function of the beam energy is different for different harmonics. For comparison, the numerical simulation data was also shown on the same figure (dots). Since η' is an oscillating function of time (see Figure 2), we have consistently chosen from the simulation data a η' which is 80 percent of the peak value. The agreement between Equation (8) and the simulation data is very good for all the nonfundamental harmonics except the second where there is a small discrepancy at lower beam energies. This is due to the fact that the energy depletion saturation mechanism, which still plays a minor role at the second harmonic, has been neglected in the analytical theory.

To summarize, we have presented a general linear dispersion relation and a concise efficiency scaling relation for the gyro-TWA. These results represent the first comprehensive analytical and simulation studies of the nonfundamental harmonic interactions. In terms of experimental applications, Equation (8) can be used to assess the feasibility of a given experimental goal and to select the optimum mode and operating parameters for achieving it, while Equation (1) can be used to calculate the properties of a gyro-TWA system, such as the bandwidth and amplification rate, etc.

REFERENCES

*Permanent Address: Science Applications, Inc., McLean, Va. 22101

1. R. Q. Twiss, Australian J. Phys. 11, 564 (1958).
2. J. Schneider, Phys. Rev. Lett. 2, 504 (1959).
3. A. V. Gaponov, Izv. Vyssh. Uchebn. Zaved., Radiofizika 2, 450 (1959) and "Addendum," Izv. Vyssh. Uchebn. Zaved., Radiofizika 2, 837 (1959).
4. K. R. Chu and J. L. Hirshfield, Phys. Fluids 21, 461 (1978).
5. V. A. Flyagin, A. V. Gaponov, M. I. Petelin, and V. K. Yulpata, IEEE Trans. Microwave Theory Tech. 25, 514 (1977).
6. J. L. Hirshfield and V. L. Granatstein, IEEE Trans. Microwave Theory Tech. 25, 522 (1977).
7. E. Ott and W. M. Manheimer, IEEE Trans. Plasma Sci. PS-3, 1 (1975).
8. H. S. Uhm, R. C. Davidson, and K. R. Chu, Phys. Fluids (in press, 1978).
9. S. Ahn and J. Y. Choe, Bull. Am. Phys. Soc. 23, 749(1978).
10. P. Sprangle and W. M. Manheimer, Phys. Fluids 18, 224 (1975).
11. P. Sprangle and A. T. Drobot, IEEE Trans. Microwave Theory Tech. 25, 528 (1977).
12. K. R. Chu, A. T. Drobot, V. L. Granatstein, and J. L. Seftor, IEEE Trans. Microwave Theory Tech. (in press, 1979).
13. A. T. Drobot and K. R. Chu, to be published.

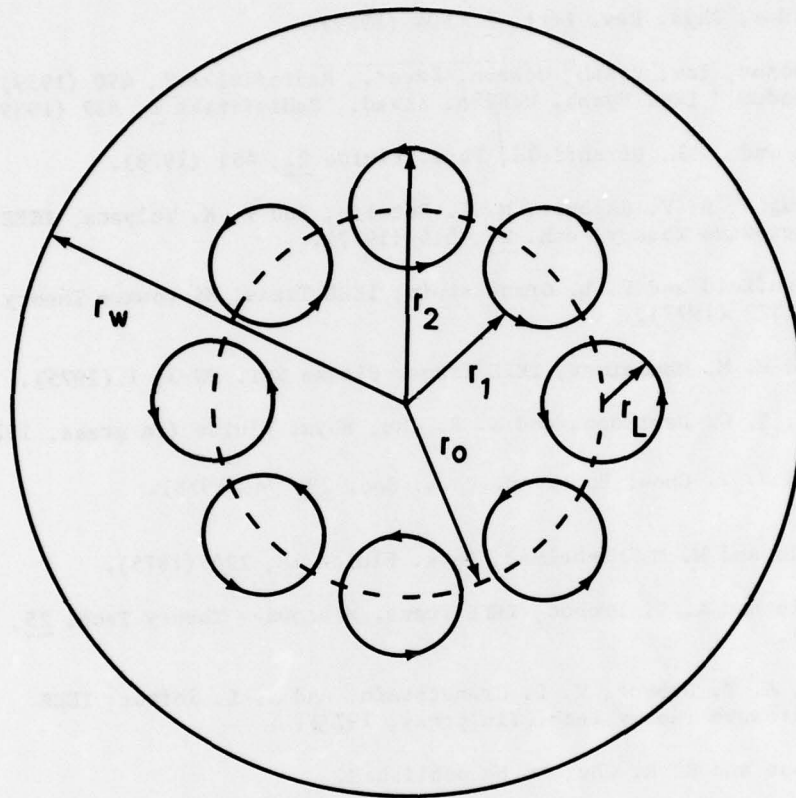


Fig. 1 - Cross-sectional view of the gyro-TWA model. The applied magnetic field (not shown) points toward the reader. The electrons are monoenergetic and all have the same Larmor radius r_L . Guiding centers of all electrons are uniformly distributed on the circle of constant radius r_0 .

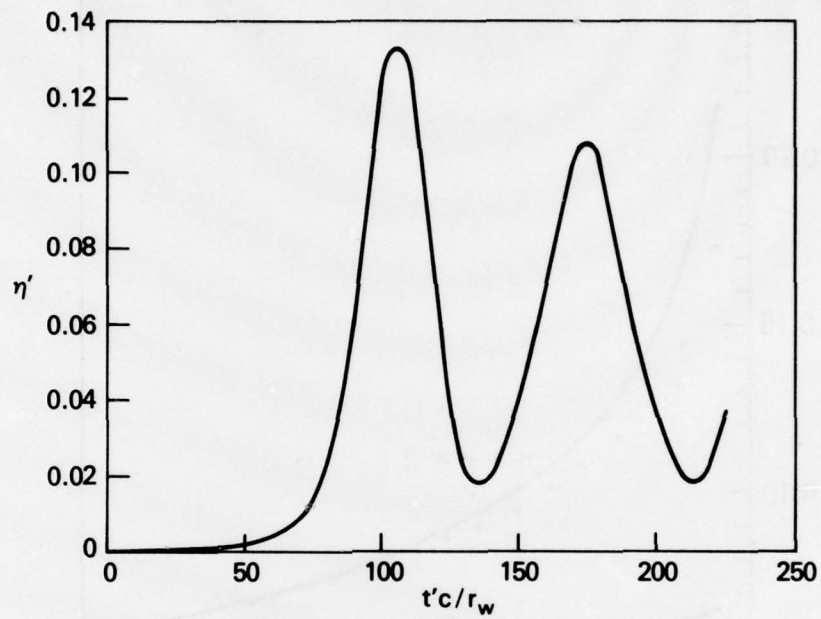


Fig. 2 - Efficiency versus time for $m=0$, $n=s=2$,
 $\nu'=0.002$, $\gamma'_o = 1.1$, and $r'_o/r_w = 0.44$

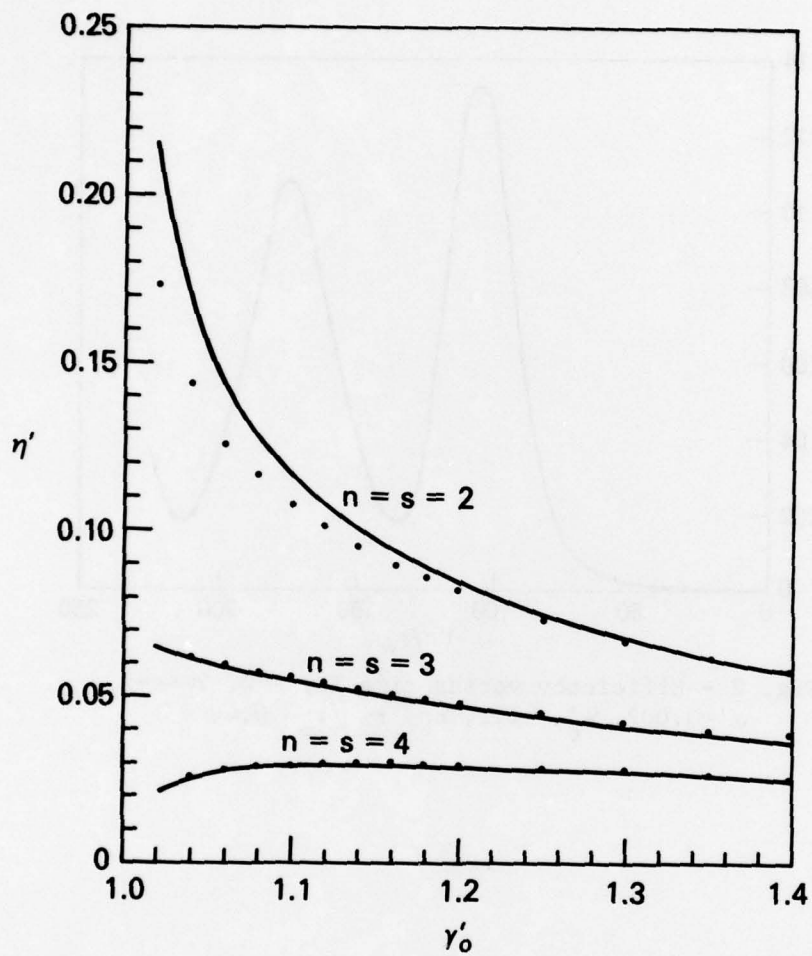


Fig. 3 - Efficiency versus beam energy for $m=0$, $\nu' = 0.002$, and optimized values of r_0 . Continuous curves are obtained from Eq. (12) and dots are simulation data.